

## Reversible Cu<sub>4</sub> ↔ Cu<sub>6</sub> Core Interconversion and Temperature Induced Single-Crystal-to-Single-Crystal Phase Transition for Copper(I) Carboxylate

Alexander S. Filatov,<sup>†</sup> Oleksandr Hietsoi,<sup>†</sup> Yulia Sevryugina,<sup>†</sup> Nikolay N. Gerasimchuk,<sup>‡</sup> and Marina A. Petrukhina<sup>\*†</sup>

<sup>†</sup>Department of Chemistry, University at Albany, 1400 Washington Avenue, Albany, New York 12222 and

<sup>‡</sup>Department of Chemistry, Missouri State University, 901 South National Avenue, Springfield, Missouri, 65897

Received October 14, 2009

The first example of a reversible [Cu<sub>4</sub>] ↔ [Cu<sub>6</sub>] interconversion for polynuclear copper(I) complexes under controlled experimental settings is reported. It illustrates the key role of specific crystal growth conditions for accessing the target cluster nuclearity that consequently determines physical properties of the resulting solid state products. Thus, when copper(I) benzoate crystallizes from a 1,2-dichlorobenzene solution at room temperature, it forms [Cu<sub>4</sub>]-core based crystalline material, [Cu<sub>4</sub>(O<sub>2</sub>CC<sub>6</sub>H<sub>5</sub>)<sub>4</sub>] (**1**). In contrast, crystal growth by deposition from the gas phase at elevated temperatures results in the exclusive formation of [Cu<sub>6</sub>(O<sub>2</sub>CC<sub>6</sub>H<sub>5</sub>)<sub>6</sub>] (**2**). Complexes **1** and **2** have been isolated in pure form, fully characterized, and reversibly interconverted into each other. The effect of a core structure on the spectroscopic properties of **1** and **2**, such as IR, Raman, and photoluminescence, has been investigated. Additionally, a combination of X-ray powder and single crystal diffraction methods has been used to discover the temperature induced phase transition in the hexanuclear copper(I) system. Two modifications of **2** exhibiting slightly different solid state packing of the [Cu<sub>6</sub>(O<sub>2</sub>CC<sub>6</sub>H<sub>5</sub>)<sub>6</sub>] units have been identified at room and low temperature. Moreover, reversible single-crystal-to-single-crystal transitions between these polymorphic forms have been confirmed. The important role of weak intermolecular interactions between polynuclear copper(I) units in the solid state has also been revealed and discussed.

### Introduction

Polynuclear complexes of copper(I), silver(I), and gold(I) are subjects of considerable research activity focused on the interplay between their geometric and electronic structures,<sup>1</sup> as well as size–reactivity relationships for practical optoelectronic,<sup>2</sup> catalytic,<sup>3</sup> and biochemical applications.<sup>4</sup> Specifically, interactions between closed d<sup>10</sup> shells in various clusters attract broad attention, since the number and arrangement of metal centers in close proximity affect stability, chemical, and photophysical

behavior of the resulting systems. However, target preparation of a desired cluster core with tailored properties remains a significant synthetic challenge. We have recently turned to investigation of polynuclear copper(I) complexes supported by various carboxylate groups since they exhibit a remarkable structural diversity and that should be the key factor allowing tuning of their physical properties and chemical reactivity. Among a rather limited number of the structurally confirmed examples, there are discrete complexes with tetra-<sup>5</sup> and hexanuclear cores,<sup>6</sup> as well as with extended structures formed by di- and tetranuclear copper units held by additional Cu···O intermolecular interactions.<sup>7,8</sup> Additionally, two new examples of extended helical chains held by cuprophilic Cu···Cu interactions in the solid state have been reported for copper(I) pivalate<sup>9</sup> and 3,5-bis(trifluoromethyl)benzoate.<sup>10</sup> Analyzing

\*Corresponding author. E-mail: marina@albany.edu.

(1) (a) Balch, A. L. *Struct. Bonding (Berlin)* **2007**, *123*, 1–40. (b) Balch, A. L. *Angew. Chem., Int. Ed.* **2009**, *48*, 2641–2644.

(2) (a) Ford, P. C.; Cariati, E.; Bourassa, J. *Chem. Rev.* **1999**, *99*, 3625–3647.

(b) Yam, V. W.-W.; Lo, K. K.-W. *Mol. Supramol. Photochem.* **1999**, 31–112. (c) Armaroli, N.; Accorsi, G.; Cardinali, F.; Listorti, A. *Top. Cur. Chem.* **2007**, *280*, 69–115. (d) Zhang, Q.; Ding, J.; Cheng, Y.; Wang, L.; Xie, Z.; Jing, X.; Wang, F. *Adv. Funct. Mater.* **2007**, *17*, 2983–2990. (e) Osawa, M.; Hoshino, M. *Chem. Commun.* **2008**, *47*, 6384–6386. (f) Barbieri, A.; Accorsi, G.; Armaroli, N. *Chem. Commun.* **2008**, *19*, 2185–2193. (g) Knorr, M.; Guyon, F.; Khatyr, A.; Däschlein, C.; Strohmman, C.; Aly, S. M.; Abd-El-Aziz, A. S.; Fortin, D.; Harvey, P. D. *Dalton Trans.* **2009**, 948–955.

(3) See *Chem. Rev.* **2008**, *108* (Coinage Metals In Organic Synthesis), 2793–3442.

(4) (a) Klinman, J. P. *Chem. Rev.* **1996**, *96*, 2541–2561. (b) Kim, E.; Chufan, E. E.; Kamaraj, K.; Karlin, K. D. *Chem. Rev.* **2004**, *104*, 1077–1133. (c) Hong, S.; Huber, S. M.; Gagliardi, L.; Cramer, C. C.; Tolman, W. B. *J. Am. Chem. Soc.* **2007**, *129*, 14190–14192. (d) Wang, J.; Schopfer, M. P.; Sarjeant, A. A. N.; Karlin, K. D. *J. Am. Chem. Soc.* **2009**, *131*, 450–451.

(5) Sevryugina, Y.; Hietsoi, O.; Petrukhina, M. A. *Chem. Commun.* **2007**, 37, 3853–3855.

(6) Sevryugina, Y.; Rogachev, A. Yu.; Petrukhina, M. A. *Inorg. Chem.* **2007**, *46*, 7870–7879.

(7) Cotton, F. A.; Dikarev, E. V.; Petrukhina, M. A. *Inorg. Chem.* **2000**, *39*, 6072–6079.

(8) Sevryugina, Y.; Vaughn, D. D., II; Petrukhina, M. A. *Inorg. Chim. Acta* **2007**, *360*, 3103–3107.

(9) Sugiura, T.; Yoshikawa, H.; Awaga, K. *Inorg. Chem.* **2006**, *45*, 7584–7586.

(10) Sevryugina, Y.; Petrukhina, M. A. *Eur. J. Inorg. Chem.* **2008**, 219–229.

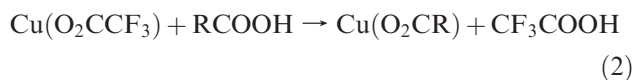
these scattered cases, one could assign a certain structural type to a specific bridging carboxylate, thus creating an illusion that the former is determined by the ligand nature. However, our recent investigation on the fragmentation of polymeric copper(I) 3,5-bis(trifluoromethyl)benzoate has provided the first system where several polynuclear  $\text{Cu}_n$ -core complexes ( $n = 2, 4, \text{ and } 6$ ) were synthesized and structurally characterized for the same carboxylate ligand.<sup>10</sup> Although crystallized as adducts with different polyaromatic donors, the isolated discrete  $\text{Cu}^{\text{I}}$  complexes of various nuclearities demonstrated that multiple polynuclear structural arrangements exist for a given carboxylate bridging group. It was also predicted that variations in the preparation or crystallization conditions should affect the resulting structural outcome. In this work, we support the above prediction by our new results obtained for copper(I) benzoate, for which two complexes of different nuclearity,  $[\text{Cu}_4(\text{O}_2\text{CC}_6\text{H}_5)_4]$  ( $[\text{Cu}_4]$ ) and  $[\text{Cu}_6(\text{O}_2\text{CC}_6\text{H}_5)_6]$  ( $[\text{Cu}_6]$ ), have been individually prepared in high yield and fully characterized by X-ray diffraction and spectroscopic techniques. Importantly, it was demonstrated that the  $[\text{Cu}_4]$  and  $[\text{Cu}_6]$  units reversibly interconvert into each other, providing a remarkable example of such transformation for discrete polynuclear copper(I) complexes. Moreover, a reversible single-crystal-to-single-crystal temperature induced phase transition was revealed for the  $[\text{Cu}_6]$ -product. Thus, this system provided a unique case to examine the effects of core structures and intermolecular interactions on the resulting spectroscopic properties, including IR, Raman, and photoluminescence.

## Results and Discussion

**Syntheses and Structures.** In general,  $\text{Cu}^{\text{I}}$  compounds have been less studied than  $\text{Cu}^{\text{II}}$  analogues due to their instability in solutions. This especially applies to the Lewis acidic complexes, in which electrophilicity at the  $\text{Cu}^{\text{I}}$  centers is enhanced by the presence of fluorinated carboxylate ligands. Thus, solution chemistry of the fluorinated benzoate copper(I) complexes was recently found to be very limited<sup>5,6,10</sup> due to facile disproportionation and oxidation reactions. The nonfluorinated analogues, however, show better stability in solution. For example, copper(I) benzoate was prepared based on the reaction 1 and crystallized from solution back in 1973.<sup>11</sup> A few years later, its structure was reported to have a tetranuclear core,  $[\text{Cu}_4(\text{O}_2\text{CC}_6\text{H}_5)_4]$  (**1**).<sup>12</sup>



To access copper(I) carboxylates, we have recently developed a different preparation scheme (2) based on the ligand-exchange procedure starting from copper(I) trifluoroacetate followed by gas phase sublimation–deposition steps for purification and crystal growth.



This path was shown to be very efficient for the synthesis of several new polynuclear copper(I) benzoates

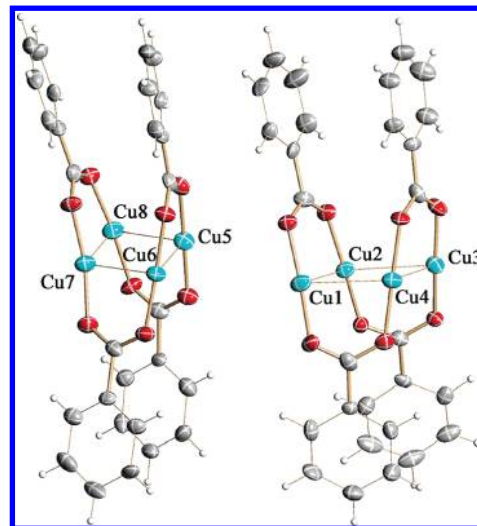


**Figure 1.** ORTEP representation of the asymmetric unit in **1** showing the Cu labeling scheme with the thermal ellipsoids drawn at the 40% probability level. Cu blue, O red, C gray, H light gray. This color scheme is used in all figures.

having fluorinated substituents,<sup>5,6,8,10</sup> since the presence of water (as a result of reaction 1) in highly electrophilic systems is not desirable. When we applied the latter synthetic approach culminated with the vapor deposition to access single crystals of copper(I) benzoate, colorless blocks (**2**) having unique unit cell parameters were isolated. Similar to **1**, their elemental analysis was consistent with a 1:1 copper-to-benzoate product composition. The X-ray structural characterization of **2** performed at 173 K revealed a different structural type, a planar hexanuclear  $[\text{Cu}_6(\text{O}_2\text{CC}_6\text{H}_5)_6]$  core instead of tetranuclear  $[\text{Cu}_4(\text{O}_2\text{CC}_6\text{H}_5)_4]$  (**1**). Thus, copper(I) benzoate provided the first example when variations in preparation/crystallization conditions yielded two different polynuclear carboxylate complexes,  $[\text{Cu}_4]$  and  $[\text{Cu}_6]$ . Therefore, we set out to carefully investigate this interesting system focusing on possible structural transformations between  $[\text{Cu}_4]$  and  $[\text{Cu}_6]$  as well as on their structure–property correlations.

**Solid-State Structure of  $[\text{Cu}_4(\text{O}_2\text{CC}_6\text{H}_5)_4]$  (**1**).** We have reproduced the synthesis and solution crystallization suggested by Edwards and co-workers<sup>11,12</sup> and have recollected the single-crystal X-ray diffraction experiment for **1** at low temperature. Importantly, X-ray powder diffraction confirmed the purity and the  $[\text{Cu}_4]$  identity of the bulk crystalline product obtained from either reaction 1 or 2, as well as after its recrystallization from 1,2-dichlorobenzene (Supporting Information Figures S5 and S9).

Copper(I) benzoate **1** crystallizes in the triclinic  $P\bar{1}$  space group with two crystallographically independent tetramers in the asymmetric unit. The latter are similar but not identical; both have a planar core comprised of four copper atoms bridged by four benzoate ligands alternating above and below the  $[\text{Cu}_4]$  plane (Figure 1).

The geometric parameters of these tetramers are very close to the data reported previously.<sup>12</sup> The intramolecular  $\text{Cu}\cdots\text{Cu}$  distances within the  $[\text{Cu}_4]$  plane range from 2.713(2) Å for  $\text{Cu}(2)\cdots\text{Cu}(3)$  to 2.748(2) Å for  $\text{Cu}(1)\cdots\text{Cu}(4)$ . For the second tetramer, these distances span from 2.718(2) Å for  $\text{Cu}(5)\cdots\text{Cu}(6)$  to 2.733(2) Å for  $\text{Cu}(5)\cdots\text{Cu}(8)$ . The average value of  $\text{Cu}\cdots\text{Cu}_{\text{carb-bridged}}$

(11) Edwards, D. A.; Richards, R. *J. Chem. Soc., Dalton Trans.* **1973**, 2463–2468.

(12) Drew, M. G. B.; Edwards, D. A.; Richards, R. *J. Chem. Soc., Dalton Trans.* **1977**, 299–303.

**Table 1.** Selected Bond Distances (Å) and Angles (deg) for  $[\text{Cu}_n(\text{O}_2\text{CR})_n]$ , R =  $\text{C}_6\text{H}_5$ , (3-F) $\text{C}_6\text{H}_4$ , (2,3,4-F) $_3\text{C}_6\text{H}_2$ , and (3,5-F) $_2\text{C}_6\text{H}_3$  ( $T = 173$  K)

R	$\text{C}_6\text{H}_5^b$	(3-F) $\text{C}_6\text{H}_4$	(2,3,4-F) $_3\text{C}_6\text{H}_2$	$\text{C}_6\text{H}_5$	(3,5-F) $_2\text{C}_6\text{H}_3$
	<b>1</b> [this work]	<b>3</b> <sup>5</sup>	<b>4</b> <sup>5</sup>	<b>2</b> [this work]	<b>5</b> <sup>6</sup>
$n$	4	4	4	6	6
$\text{Cu}\cdots\text{Cu}_{\text{carb-bridged}}$	2.746(2)/2.718(2) 2.713(2)/2.718(2) 2.725(2)/2.723(2) 2.748(2)/2.733(2)	2.712(1) 2.728(1)	2.690(1)	2.679(1) 2.693(1) 2.723(1)	2.706(1) 2.722(1) 2.826(1)
$\text{Cu}\cdots\text{Cu}_{\text{nonbridged}}$	2.904(2)/3.125(2) 4.630(2)/4.460(2)	2.879(2) 4.614(2)	2.927(1) 4.513(1)	2.981(1) 3.051(1) 4.704(1)	2.962(1) 2.962(1) 3.189(1)
$\text{Cu}-\text{O}_{\text{carb}}^a$	1.865(7)/1.858(8)	1.857(4)	1.853(2)	1.863(2)	1.851(3)
$\text{Cu}\cdots\text{Cu}_{\text{intermol}}$	3.239(2) 3.547(2)				
$\text{Cu}\cdots\text{O}_{\text{intermol}}$	3.098(8)-3.468(8)				
$\text{Cu}-\text{Cu}-\text{Cu}$	64.57(5)/70.19(6) 115.57(7)/109.82(7) 63.83(5)/69.89(6) 116.00(7)/110.10(7)	63.91(3) 116.03(3)	65.94(2) 114.06(2)	67.39(2) 120.55(2) 171.92(2)	66.15(2) 123.48(3) 170.27(3)

<sup>a</sup> Averaged. <sup>b</sup> Two crystallographically independent units.

separations in **1** of 2.728(2) Å is within the sum of the van der Waals radii generally accepted for copper ( $r_{\text{vdW}}(\text{Cu}) = 1.40$  Å).<sup>13</sup> It is noteworthy that the  $r_{\text{vdW}}$  value for copper was recently re-evaluated to be much longer, namely 1.92 Å.<sup>14</sup> Additional  $\text{Cu}\cdots\text{Cu}$  contacts between the non-bridged metal centers within the  $[\text{Cu}_4]$  cores (2.904(2) Å for  $\text{Cu}(2)\cdots\text{Cu}(4)$  and 3.125(2) Å for  $\text{Cu}(5)\cdots\text{Cu}(7)$ ) can be mentioned. This tetrameric core is not unique and has recently been found in two other discrete copper(I) carboxylate complexes, namely  $[\text{Cu}_4(\text{O}_2\text{C}(3\text{-F})\text{C}_6\text{H}_4)_4]$  (**3**) and  $[\text{Cu}_4(\text{O}_2\text{C}(2,3,4\text{-F})_3\text{C}_6\text{H}_2)_4]$  (**4**) (Table 1).<sup>5</sup>

The above-mentioned  $[\text{Cu}_4]$  complexes bearing fluorinated benzoates crystallize in the higher symmetry space groups than **1** ( $C2/c$  and  $Fddd$  for **3** and **4**, respectively). Furthermore, all sides of the  $[\text{Cu}_4]$ -core in **4** are equal (Table 1). Apart from the symmetry considerations, the tetranuclear complexes **1**, **3**, and **4** have similar molecular geometries. However, when checking the packing of tetramers in **1**, we found interesting features that were overlooked in the past.<sup>12</sup> Several types of intermolecular interactions in the solid-state structure of **1** deserve to be mentioned. First, there is an alignment of individual tetra-copper units (Figure 2) with the shortest intermolecular  $\text{Cu}(3)\cdots\text{Cu}(6)$  separation being 3.239(2) Å. The  $\text{Cu}(4)\cdots\text{Cu}(5)$  contact of 3.547(2) Å is longer. The corresponding  $\text{Cu}(7)-\text{Cu}(6)-\text{Cu}(3)$  and  $\text{Cu}(8)-\text{Cu}(5)-\text{Cu}(4)$  angles are 162.35(7) and 172.30(7)°. Second, four Cu atoms of the two tetramers that are not involved in intermolecular cuprophilic interactions exhibit  $\text{Cu}\cdots\pi(\text{C}_6\text{H}_5)$  contacts ranging from 3.21 to 3.70 Å. Thus, the crystal packing of  $[\text{Cu}_4]$  units along the crystallographic  $a$  axis is based on alternating weak intermolecular  $\text{Cu}\cdots\text{Cu}$  and  $\text{Cu}\cdots\pi$  interactions. Third, there are no intermolecular cuprophilic interactions along the crystallographic  $b$  axis. Instead, they are replaced by  $\text{Cu}\cdots\text{O}$  contacts (3.10–3.47 Å) with weak  $\text{Cu}\cdots\pi$  interactions (3.17–3.73 Å) also being present. All these intermolecular contacts are within or close to the sums of the van der Waals radii for copper and oxygen or carbon ( $r_{\text{vdW}}(\text{Cu}, \text{O}) = 3.44$  Å and  $r_{\text{vdW}}(\text{Cu}, \text{C}) = 3.69$  Å)<sup>14</sup> and,

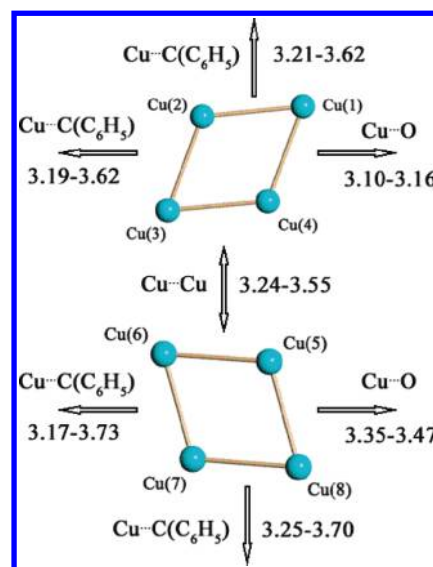


**Figure 2.** Schematic representation of intermolecular contacts (Å) in the solid-state structure of  $[\text{Cu}_4(\text{O}_2\text{CC}_6\text{H}_5)_4]$  (**1**).

thus, may affect the physical properties of the crystalline products. Importantly, intermolecular interactions of the  $\text{Cu}\cdots\text{Cu}$  and  $\text{Cu}\cdots\text{O}$  types are absent in the solid state structures of  $[\text{Cu}_4(\text{O}_2\text{C}(3\text{-F})\text{C}_6\text{H}_4)_4]$  and  $[\text{Cu}_4(\text{O}_2\text{C}(2,3,4\text{-F})_3\text{C}_6\text{H}_2)_4]$ . At the same time, the similarly long (3.23–3.48 Å)  $\text{Cu}\cdots\pi$  contacts can be identified in both **3** and **4**.

**Solid-State Structure of  $[\text{Cu}_6(\text{O}_2\text{CC}_6\text{H}_5)_6]$  (**2**,  $T = 173$  K).** Copper(I) benzoate (**2**) crystallizes in the triclinic  $P\bar{1}$  space group with one-half of the  $[\text{Cu}_6(\text{O}_2\text{CC}_6\text{H}_5)_6]$  moiety being crystallographically independent. The  $[\text{Cu}_6(\text{O}_2\text{CC}_6\text{H}_5)_6]$  molecule resides on an inversion center positioned in the middle of its core. A planar hexagon is comprised of six copper atoms bridged by six benzoate ligands alternating above and below the plane (Figure 3). The hexanuclear core structure was first seen in copper(I) 3,5-difluorobenzoate (**5**)<sup>6</sup> and was later found in the polyarene adducts of copper(I) 3,5-bis(trifluoromethyl)benzoate.<sup>10,15</sup>

(13) Bondi, A. J. *Phys. Chem.* **1964**, *68*, 441–451.

(14) (a) Batsanov, S. S. *Inorg. Mater.* **2001**, *37*, 871–885. (b) Nag, S.; Banerjee, K.; Datta, D. *New J. Chem.* **2007**, *31*, 832–834.

(15) Sevryugina, Y.; Jackson, E. A.; Scott, L. T.; Petrukhina, M. A. *Inorg. Chim. Acta* **2008**, *361*, 3103–3108.

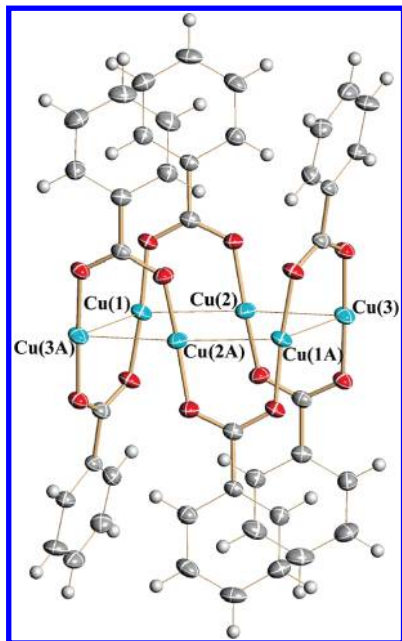


**Figure 3.** ORTEP representation of the  $[\text{Cu}_6(\text{O}_2\text{CC}_6\text{H}_5)_6]$  complex showing the Cu labeling scheme with thermal ellipsoids drawn at the 40% probability level. Symmetry operation:  $-x + 1, -y, -z + 1$ .

The  $\text{Cu}\cdots\text{Cu}$  distances within the  $[\text{Cu}_6]$  core in **2** range from 2.6797(6) Å for  $\text{Cu}(2)\cdots\text{Cu}(3)$  to 2.7231(6) Å for  $\text{Cu}(1)\cdots\text{Cu}(2)$ . The interior angles are 171.92(2)° for  $\text{Cu}(1)-\text{Cu}(2)-\text{Cu}(3)$ , 120.549(19)° for  $\text{Cu}(2)-\text{Cu}(1)-\text{Cu}(3\text{A})$ , and 67.390(16)° for  $\text{Cu}(2)-\text{Cu}(3)-\text{Cu}(1\text{A})$ . This results in additional short  $\text{Cu}\cdots\text{Cu}$  contacts between the nonbridged metal centers,  $\text{Cu}(2)\cdots\text{Cu}(2\text{A})$  of 3.0514(8) Å, and  $\text{Cu}(1)\cdots\text{Cu}(2\text{A})$  of 2.9812(6) Å. The average  $\text{Cu}-\text{O}_{\text{carb}}$  distance of 1.863(2) Å in **2** is similar to those in **1** and **5** (1.861(7) and 1.851(3) Å, respectively).

A comparison of the molecular  $[\text{Cu}_6]$  cores in analogous complexes with benzoate and 3,5-difluorobenzoate bridges shows a close similarity with small variations in copper–copper distances and angles (Table 1). In the solid state, both  $[\text{Cu}_6]$  complexes are not engaged in either  $\text{Cu}\cdots\text{O}$  or  $\text{Cu}\cdots\text{Cu}$  intermolecular interactions. The shortest  $\text{Cu}\cdots\text{O}$  distance found in **2** is 4.088(2) Å, while the shortest intermolecular  $\text{Cu}\cdots\text{Cu}$  separation is 5.9621(7) Å. This contrasts the intermolecular contacts found in **1** and, importantly, allows a rationalization of different photophysical properties of **1** and **2**, as discussed below. At the same time, weak intermolecular  $\text{Cu}\cdots\pi$  interactions (3.01–3.72 Å) can be identified in the solid-state structures of **2** and **5**, similarly to those found in  $[\text{Cu}_4]$  core complexes with aromatic carboxylate bridges. Small variations in packing of the  $[\text{Cu}_6]$  units related to a different engagement of copper(I) atoms in  $\text{Cu}\cdots\pi$  interactions are found in **2** and **5** (see the Supporting Information for details) and that may perturb their electronic structures and thus affect the photoluminescent properties of the crystalline materials.

**Temperature-Induced Reversible Single-Crystal-to-Single-Crystal Phase Transition for 2.** To confirm the identity of the bulk crystalline product **2**, we relied on the X-ray powder diffraction method. To our surprise, the experimental spectrum recorded for single crystals of  $[\text{Cu}_6(\text{O}_2\text{CC}_6\text{H}_5)_6]$  at room temperature showed no consistency

with the simulated pattern based on the unit cell parameters obtained for **2** at 173 K (Supporting Information Figure S6). However, when multiple crystals were rechecked again by single crystal X-ray diffraction at 173 K, they all conformed to the same unit cell parameters found for **2**<sub>173K</sub>. Puzzled by these facts, we have recollected the single crystal diffraction experiment for **2** at room temperature and found a different set of unit cell parameters (**2**<sub>293K</sub>, Table 2). The structure solution of **2**<sub>293K</sub> revealed that its molecular building unit is a  $[\text{Cu}_6(\text{O}_2\text{CC}_6\text{H}_5)_6]$  complex similar to that in **2**<sub>173K</sub>. In contrast to the low temperature modification, however, there are two crystallographically independent hexanuclear complexes in the asymmetric unit of **2**<sub>293K</sub>. This results in the slightly different crystal packing of the  $[\text{Cu}_6]$  units at low and room temperatures (Figure 4).

While all major bond distances and angles of the hexacopper(I) complexes in **2**<sub>293K</sub> closely resemble those in **2**<sub>173K</sub>, some variations in the atom positioning affect their overall arrangement in the solid state and result in the observed temperature induced phase transition. The above changes seem subtle and do not cause the crystal degradation, thus providing a possibility to study both phases by single crystal X-ray diffraction. It was found that conversion between the two phases is fully reversible and occurs between 263 and 253 K. After repeating the cooling–thawing cycles from 293 to 173 K three times for the same crystal, the single crystal diffraction data showed only a minor degradation of the crystal quality in comparison with the previously collected data at the same temperature (Table S1 of the Supporting Information). Although the topochemical reactions in solid state are well-documented,<sup>16</sup> the single-crystal-to-single-crystal phase transitions are rare and commonly accompanied by problems associated with very weak high-angle scattering and/or substantially increased mosaicity of crystals.<sup>17</sup> Moreover, reversible phase transitions between discrete molecular structures are exceptional,<sup>18</sup> perhaps due to the fact that cooperative molecular rearrangements in such systems are rarely accompanied by retention of the overall structural integrity. In contrast, the temperature- and guest-induced single-crystal-to-single-crystal transformations are relatively common in rigid coordination polymers<sup>19</sup> and metal–organic frameworks.<sup>20</sup> It is worth stressing

(16) (a) Friscic, T.; MacGillivray, L. R. *Z. Kristallogr.* **2005**, *220*, 351–363. (b) Garcia-Garibay, M. A. *Angew. Chem., Int. Ed.* **2007**, *46*, 8945–8947. (c) MacGillivray, L. R.; Papaefstathiou, G. S.; Friscic, T.; Hamilton, T. D.; Bucar, D.-K.; Chu, Q.; Varshney, D. B.; Georgiev, I. G. *Acc. Chem. Res.* **2008**, *41*, 280–291. (d) Lauher, J. W.; Fowler, F. W.; Goroff, N. S. *Acc. Chem. Res.* **2008**, *41*, 1215–1229.

(17) (a) Ma, J. P.; Dong, Y.-B.; Huang, R.-Q.; Smith, M. D.; Su, C.-Y. *Inorg. Chem.* **2005**, *44*, 6143–6145. (b) Zhang, Y.-J.; Liu, T.; Kanegawa, S.; Sato, O. *J. Am. Chem. Soc.* **2009**, *131*, 7942–7943.

(18) (a) Evers, J.; Klapotke, T. M.; Mayer, P.; Oehlinger, G.; Welch, J. *Inorg. Chem.* **2006**, *45*, 4996–5007. (b) For a nonreversible phase transition between discrete complexes, see: Mobin, S. M.; Srivastava, A. K.; Mathur, P.; Lahiri, G. K. *Inorg. Chem.* **2009**, *48*, 4652–4654.

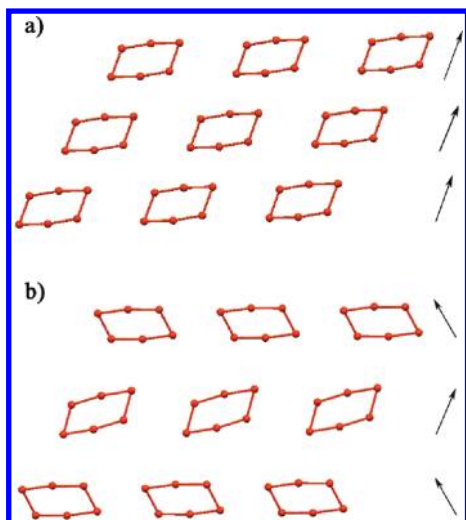
(19) (a) Wang, X.-Y.; Scancella, M.; Sevov, S. C. *Chem. Mater.* **2007**, *19*, 4506–4513. (b) Vittal, J. J. *Coord. Chem. Rev.* **2007**, *251*, 1781–1795. (c) Kawano, M.; Fujita, M. *Coord. Chem. Rev.* **2007**, *251*, 2592–2605.

(20) (a) Suh, M. P.; Cheon, Y. E. *Aust. J. Chem.* **2006**, *59*, 605–612. (b) Lee, J. Y.; Lee, S. Y.; Sim, W.; Park, K.-M.; Kim, J.; Lee, S. S. *J. Am. Chem. Soc.* **2008**, *130*, 6902–6903. (c) Bernini, M. C.; Gandara, F.; Iglesias, M.; Snejko, N.; Gutierrez-Puebla, E.; Brusau, E. V.; Narda, G. E.; Monge, M. A. *Chem.—Eur. J.* **2009**, *15*, 4896–4905. (d) Montney, M. R.; Supkowski, R. M.; Staples, R. J.; LaDuca, R. L. *J. Solid State Chem.* **2009**, *182*, 8–17.

**Table 2.** Crystallographic Data and X-ray Experimental Conditions for  $\text{Cu}_n(\text{O}_2\text{CC}_6\text{H}_5)_n$  ( $n = 4, 6$ )

<i>n</i>	4 [this work]	6 [this work]	6 [this work]	
	4 <sup>[12]</sup>	1	2 <sub>173K</sub>	2 <sub>293K</sub>
empirical formula	$\text{C}_{28}\text{H}_{20}\text{Cu}_4\text{O}_8$	$\text{C}_{28}\text{H}_{20}\text{Cu}_4\text{O}_8$	$\text{C}_{42}\text{H}_{30}\text{Cu}_6\text{O}_{12}$	$\text{C}_{42}\text{H}_{30}\text{Cu}_6\text{O}_{12}$
formula weight	740.08	738.60	1107.90	1107.90
<i>T</i> (K)	283–303	173(2)	173(2)	293(2)
crystal description		elongated plate	block	block
crystal color		colorless	colorless	colorless
crystal system	triclinic	triclinic	triclinic	triclinic
space group	$P\bar{1}$	$P\bar{1}$	$P\bar{1}$	$P\bar{1}$
<i>a</i> (Å)	15.408(7)	13.4736(12)	9.2520(7)	11.5075(17)
<i>b</i> (Å)	13.784(12)	14.9872(13)	9.6674(7)	13.189(2)
<i>c</i> (Å)	15.034(9)	15.3365(13)	11.2642(8)	13.933(2)
$\alpha$ (deg)	92.43(6)	62.6130(10)	107.5690(10)	95.643(2)
$\beta$ (deg)	62.34(5)	67.9140(10)	90.6550(10)	102.960(2)
$\gamma$ (deg)	112.71(6)	87.182(2)	92.0470(10)	95.054(2)
<i>V</i> (Å <sup>3</sup> )	2571.981	2519.0(4)	959.63(12)	2037.5(5)
<i>Z</i>	4	4	1	2
<i>D</i> <sub>calcd</sub> (g/cm <sup>3</sup> )		1.948(1)	1.917(1)	1.806(1)
<i>R</i> 1 <sup>a</sup> , <i>wR</i> 2 <sup>b</sup> [ <i>I</i> > 2σ( <i>I</i> )]	0.064	0.0721, 0.1259	0.0375, 0.0883	0.0565, 0.1369
<i>R</i> 1 <sup>a</sup> , <i>wR</i> 2 <sup>b</sup> (all data)		0.2112, 0.2167	0.0561, 0.0961	0.1090, 0.1660
quality-of-fit <sup>c</sup>		1.016	1.012	1.004
largest diff. peak/hole, e/Å <sup>3</sup>		0.933/1.169	0.581/0.361	1.065/0.532

<sup>a</sup>*R*1 =  $\sum||F_o| - |F_c||/\sum|F_o|$ . <sup>b</sup>*wR*2 =  $[\sum[w(F_o^2 - F_c^2)^2]/\sum[w(F_o^2)^2]]^{1/2}$ . <sup>c</sup>Quality-of-fit =  $[\sum[w(F_o^2 - F_c^2)^2]/(N_{\text{obs}} - N_{\text{params}})]^{1/2}$ , based on all data.

**Figure 4.** Fragment of the crystal packing of the  $[\text{Cu}_6]$  units at (a) 173 and (b) 293 K. Benzoate groups are omitted for clarity.

here that temperature induced phase transitions should be taken into account when examining the solid state properties of bulk crystalline materials and considering their structure–property relationships. On many occasions, there is a mismatch between the property measurements (often done at room temperatures) and single crystal diffraction data (usually collected at low temperatures) used for structural assignments and correlations. In these cases, X-ray powder diffraction should be used as an indispensable tool to rule out the possibility of phase transformations in addition to confirming the full structural match of selected single crystals and bulk materials.

The reversible single-crystal-to-single-crystal phase transition found in  $[\text{Cu}_6(\text{O}_2\text{CC}_6\text{H}_5)_6]$  allowed us to test if the observed changes in the solid state packing affect bulk properties of the same molecular complex (see Photoluminescent Properties).

**$[\text{Cu}_4] \leftrightarrow [\text{Cu}_6]$  Core Transformations.** We have reproducibly obtained individual copper(I) benzoate complexes **1** and **2** having different core nuclearities under controlled experimental conditions. The  $[\text{Cu}_4]$  product crystallizes from solution (xylene, dichlorobenzene) at room temperature, while the  $[\text{Cu}_6]$  crystals deposit from the gas phase at elevated temperatures under reduced pressure. The X-ray powder diffraction data have confirmed the structural identity and purity of both bulk crystalline materials. For the next step, we applied sublimation–deposition procedures to the single crystals of  $[\text{Cu}_4]$  and completely converted those to  $[\text{Cu}_6]$ . Similarly, when crystals of  $[\text{Cu}_6]$  are redissolved and then recrystallized from dichlorobenzene, they quantitatively transform back to  $[\text{Cu}_4]$ . These conversion procedures can be repeated multiple times, confirming a reversible transformation in the  $[\text{Cu}_4] \leftrightarrow [\text{Cu}_6]$  system, depending on the crystallization conditions.

Thermogravimetric analysis of  $[\text{Cu}_4]$  and  $[\text{Cu}_6]$  shows very similar patterns for **1** and **2** (Figures S12 and S15 of the Supporting Information). The weight loss commences at ca. 150 °C corresponding to the cleavage of carboxylate groups and some partial sublimation of compounds under the dinitrogen flow. After the initial weight loss, the plateau is observed and the final decomposition product corresponds to 42% of the mass residue. This is confirmed by X-ray powder diffraction to be copper(I) monooxide ( $\text{Cu}_2\text{O}$ ) in **1** and **2**. The thermal behavior of both complexes was also studied by differential scanning calorimetry (Figures S13, S14, and S16). The thermograph for  $[\text{Cu}_6]$  is featureless up to ca. 260 °C at which the sharp endothermic peak is observed and attributed to the product melting followed by decomposition. In contrast, the thermograph of  $[\text{Cu}_4]$  shows a broad exothermic peak at 200–225 °C before the product melting and thermal decomposition at ca. 260–270 °C. This peak corresponds to the transformation of  $[\text{Cu}_4]$  to  $[\text{Cu}_6]$ , as confirmed by the X-ray powder diffraction experiments (Figure S8). When the sample of  $[\text{Cu}_4]$  was heated at 150 °C for 20 days

in a sealed ampule, no phase changes were observed, while increasing temperature to 200 °C led to appearance of the [Cu<sub>6</sub>] phase. We can only speculate that this transformation proceeds through local sublimation, gas phase core rearrangement and ligand redistribution, and crystallization sequence based on the fact that this process is exothermic. It seems rather improbable that such drastic structural changes may occur in the solid state only, and in the case of the melt reaction, the endothermic peak should have been observed.<sup>21</sup>

Such reversible interconversions between molecular structures of the same composition are rather unique; the other examples for the metal carboxylate family include the triangle-to-square transformations of dirhodium(II) oxalate<sup>22</sup> and dimolybdenum(II) perfluoroterephthalate.<sup>23</sup> Lippard and co-workers have recently reported a reversible interconversion where the use of different solvents for crystallization led to the isolation of iron(II) carboxylate complexes with different nuclearities.<sup>24</sup> The formation of dinuclear and hexanuclear copper(II) pivalates that seemed to be dependent on the basicity and coordinating ability of the base employed in the reaction can also be mentioned here.<sup>25</sup> It should be emphasized that in contrast to interconversions involving discrete molecular complexes, the monomer–oligomer–polymer transformations are very common among the coordination polymers. For example, solvent-dependent interconverting systems were reported for coinage,<sup>26</sup> d-transition,<sup>27</sup> and lanthanide metal ions.<sup>28</sup>

**Spectroscopic Characterization of [Cu<sub>4</sub>(O<sub>2</sub>CC<sub>6</sub>H<sub>5</sub>)<sub>4</sub>] (1) and [Cu<sub>6</sub>(O<sub>2</sub>CC<sub>6</sub>H<sub>5</sub>)<sub>6</sub>] (2).** The controlled preparation of **1** and **2**, having different copper(I) core structures bridged

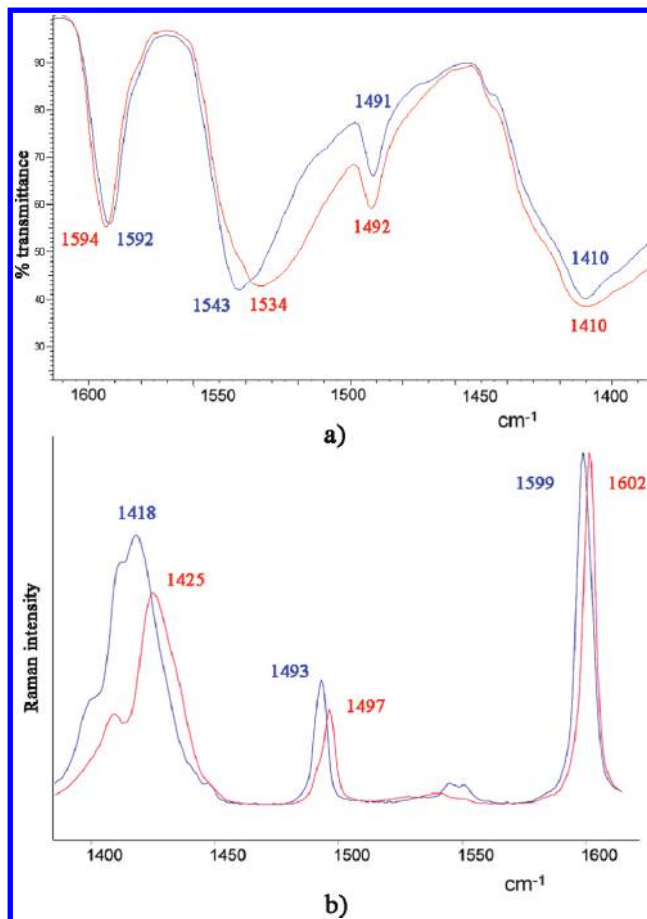


**Figure 5.** (a) IR and (b) Raman spectra of [Cu<sub>4</sub>] (red) and [Cu<sub>6</sub>] (blue) in the carboxylate stretching region.

by the same benzoate ligands, allowed us to examine the effect of their molecular geometry and crystal packing on spectroscopic and photophysical properties.

**IR and Raman.** Infrared and Raman vibrational spectroscopies have been extensively used for structural identification of metal–ligand complexes<sup>29</sup> and proved to be powerful methods for characterization of small structural variations in coinage metal complexes.<sup>30</sup> Thus, Raman spectroscopy allowed differentiation of four Cu<sup>II</sup> acetate structures in aqueous solution, namely protonated, free, pseudobridging between a water proton and a copper ion, and bidentate.<sup>31</sup>

The solid state IR and Raman spectra of **1** and **2** are nearly identical although most bands resulting from the same vibrational modes are shifted ( $\Delta = 1\text{--}10\text{ cm}^{-1}$ ). Despite the apparent similarities of the vibrational patterns of the [Cu<sub>4</sub>] and [Cu<sub>6</sub>] complexes, it is informative to closely look at the carboxylate stretching region in both types of spectra (Figure 5). The main difference in the infrared spectra involves the symmetric CO stretch that shows up at 1543 cm<sup>-1</sup> in **2** but is shifted by 9 cm<sup>-1</sup> to the lower energy in **1**. This may be a result of different intermolecular interactions found in the solid-state structures of two copper(I) benzoates. As mentioned above, the additional Cu···O interactions are found in **1** but are absent in **2**. In the Raman spectrum of **1**, all peaks are noticeably shifted to higher energy by 3–7 cm<sup>-1</sup>

(21) Kaftory, M.; Botoshansky, M.; Kapon, M.; Shteiman, V. *Acta Crystallogr.* **2001**, B57, 791–799.

(22) Cotton, F. A.; Daniels, L. M.; Lin, C.; Murillo, C. A. *J. Am. Chem. Soc.* **1999**, 121, 4538–4539.

(23) Cotton, F. A.; Murillo, C. A.; Yu, R. *Dalton Trans.* **2006**, 3900–3905.

(24) Reisner, E.; Telser, J.; Lippard, S. J. *Inorg. Chem.* **2007**, 46, 10754–10770.

(25) Mikuriya, M.; Azuma, H.; Nukada, R.; Handa, M. *Chem. Lett.* **1999**, 57–58.

(26) (a) Matsumoto, N.; Motoda, Y.; Matsuo, T.; Nakashima, T.; Re, N.; Dahan, F.; Tuchagues, J.-P. *Inorg. Chem.* **1999**, 38, 1165–1173. (b) Chandrasekaran, P.; Mague, J. T.; Balakrishna, M. S. *Inorg. Chem.* **2006**, 45, 6678–6683. (c) Liu, H.-J.; Hung, Y.-H.; Chou, C.-C.; Su, C.-C. *Chem. Commun.* **2007**, 495–497. (d) Heo, J.; Jeon, Y.-M.; Mirkin, C. A. *J. Am. Chem. Soc.* **2007**, 129, 7712–7713. (e) Stadler, A.-M.; Kyritsakas, N.; Vaughan, G.; Lehn, J.-M. *Chem.—Eur. J.* **2007**, 13, 59–68.

(27) (a) Ramirez, J.; Stadler, A.-M.; Kyritsakas, N.; Lehn, J.-M. *Chem. Commun.* **2007**, 237–239. (b) Uehara, K.; Kasai, K.; Mizuno, N. *Inorg. Chem.* **2007**, 46, 2563–2570. (c) Kang, H. J.; Noh, T. H.; Jin, J. S.; Jung, O.-S. *Inorg. Chem.* **2008**, 47, 5528–5530. (d) Weilandt, T.; Troff, R. W.; Saxell, H.; Rissanen, K.; Schalley, C. A. *Inorg. Chem.* **2008**, 47, 7588–7598.

(28) (a) Mamula, O.; Lama, M.; Stoeckli-Evans, H.; Shova, S. *Angew. Chem., Int. Ed.* **2006**, 45, 4940–4944. (b) Lama, M.; Mamula, O.; Kottas, G. S.; De Cola, L.; Stoeckli-Evans, H.; Shova, S. *Inorg. Chem.* **2008**, 47, 8000–8015.

(29) Nakamoto, K. *Infrared and Raman Spectra of Inorganic and Coordination Compounds Part. B. Applications in Coordination, Organometallic, and Bioinorganic Chemistry*, 5th Ed.; John Wiley & Sons, Ltd.: New York, 1997.

(30) (a) Bott, R. C.; Bowmaker, G. A.; Davis, C. A.; Hope, G. A.; Jones, B. E. *Inorg. Chem.* **1998**, 37, 651–657. (b) Zhang, Q.; Cao, R.; Hong, M.; Wu, D.; Zhang, W.; Zhen, Y.; Liu, H. *Inorg. Chim. Acta* **1998**, 271, 93–98. (c) Alvarez, M. L.; Ai, J.; Zumft, W.; Sanders-Loehr, J.; Dooley, D. M. *J. Am. Chem. Soc.* **2001**, 123, 576–587. (d) Hagadorn, J. R.; Zahn, T. I.; Que, L., Jr.; Tolman, W. B. *Dalton Trans.* **2003**, 1790–1794. (e) Vorontsov, I. I.; Kovalevsky, A. Yu.; Chen, Y.-S.; Graber, T.; Gembicky, M.; Novozhilova, I. V.; Omary, M. A.; Coppens, P. *Phys. Rev. Lett.* **2005**, 94, 193003–1–193003–4. (f) Phillips, D. L.; Che, C.-M.; Leung, K. H.; Mao, Z.; Tse, M.-C. *Coord. Chem. Rev.* **2005**, 249, 1476–1490. (g) Kato, C. N.; Mori, W. C. R. *Chimie* **2007**, 10, 284–294. (h) Dias, H. V. R.; Flores, J. A.; Wu, J.; Kroll, P. *J. Am. Chem. Soc.* **2009**, 131, 11249–11255.

(31) Quiles, F.; Burneau, A. *Vib. Spectrosc.* **1998**, 16, 105–117.

compared to **2**. Thus, the solid  $[\text{Cu}_4]$  and  $[\text{Cu}_6]$  benzoate complexes can be distinguished by their IR and Raman spectra, although their X-ray powder diffraction identification is more straightforward.

**Photoluminescent Properties.** Although the first reports on fluorescence of aliphatic copper(I) carboxylates appeared in the literature about 30 years ago,<sup>32</sup> there have been no follow-up studies on the origin of photoluminescence (PL) or structure–property relationship for this class of compounds. The emission maxima of copper(I) formate, acetate, propionate, butyrate, valerate, hexanoate, and heptanoate were found to vary in the broad range of 535–660 nm at room temperature ( $\lambda_{\text{ex}} = 305\text{--}325$  nm), but those were not correlated with the structures of complexes.<sup>32</sup> We have recently found that the emission wavelengths for the structurally similar discrete tetranuclear complexes,  $[\text{Cu}_4(\text{O}_2\text{C}(3\text{-F})\text{C}_6\text{H}_4)_4]$  (**3**) and  $[\text{Cu}_4(\text{O}_2\text{C}(2,3,4\text{-F})_3\text{C}_6\text{H}_2)_4]$  (**4**), are very close.<sup>5</sup> In the solid state, upon exposure to UV radiation ( $\lambda_{\text{ex}} = 350$  nm), both compounds exhibited broad emission bands centered at 502 and 507 nm, respectively. In contrast, the PL measurements for solid tetranuclear copper benzoate,  $[\text{Cu}_4(\text{O}_2\text{CC}_6\text{H}_5)_4]$  (**1**), revealed an emission being significantly red-shifted to 676 nm ( $\lambda_{\text{ex}} = 418$  nm). This may result from an essential difference of the solid-state structure of **1** exhibiting intermolecular copper–copper and copper–oxygen interactions between the tetramers. Importantly, the latter interactions are absent in the structures of **3** and **4**. We have previously observed that the emission wavelength of the tetranuclear carboxylates shows a dependence on the general structural type (discrete clusters vs. extended motifs). For example, in contrast to the above-mentioned **3** and **4** having discrete tetranuclear cores, the polymeric complexes built on strong axial  $\text{Cu}\cdots\text{O}$  interactions between the tetramers,  $[\text{Cu}_4(\text{O}_2\text{CCF}_3)_2(\text{O}_2\text{CC}_6\text{F}_5)_2]_\infty$  and  $[\text{Cu}_4(\text{O}_2\text{CCF}_3)_4]_\infty$ , both display emission red-shifted to 583 nm ( $\lambda_{\text{ex}} = 350$  nm).<sup>5</sup> In this work again, we observe possible implications of copper–copper and copper–oxygen intermolecular interactions on the photophysical properties of tetramers.

The emission maxima,  $\lambda_{\text{max}}$ , of the crystalline solid sample of  $[\text{Cu}_6(\text{O}_2\text{CC}_6\text{H}_5)_6]$  (**2**) is 577 nm at room temperature ( $\lambda_{\text{ex}} = 350$  nm). For comparison, the structurally similar hexanuclear copper(I) 3,5-difluorobenzoate,  $[\text{Cu}_6(\text{O}_2\text{C}(3,5\text{-F})_2\text{C}_6\text{H}_3)_6]$  (**5**), exhibits photoluminescence at ca. 554 nm ( $\lambda_{\text{ex}} = 350$  nm) in the solid state.<sup>6</sup> Although the molecular  $[\text{Cu}_6]$  core structures of **2** and **5** are quite similar, the observed shift in emission can stem from electronic structure variations caused by different bridging carboxylate groups and also from small variations in their crystal packing patterns (see the Supporting Information for details).

The revealed phase transition in **2** as well as experimental observations that solid-state photophysical properties strongly correlate with molecular packing<sup>33</sup> and can be significantly different for different polymorphs<sup>1</sup> forced us to look closely at PL of  $[\text{Cu}_6]$  at variable temperatures. While a noticeable increase in emission intensity was

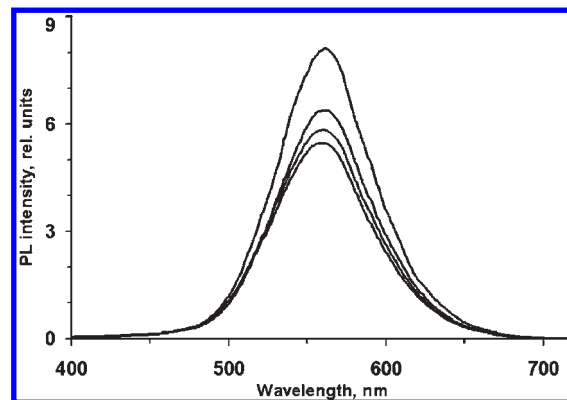


**Figure 6.** Variable temperature PL spectra of solid sample **2** taken at 0 (bottom curve),  $-29$ ,  $-55$ , and  $-83$  °C (top curve).

observed with a temperature decrease from 0 to  $-83$  °C, the overall shift in peak position constituted only 2–3 nm ( $\lambda_{\text{ex}} = 260$  nm) and can be considered negligible (Figure 6). The range from 0 to  $-30$  °C, where phase transition for **2** was structurally detected, was carefully examined (measured at every 2–3 °C from 0 to  $-40$  °C), but subtle differences in packing of the  $[\text{Cu}_6]$  units seems show no effect on the electronic communication between Cu(I) centers in this case.

## Conclusions

In summary, two different copper(I) core complexes with the same bridging ligand,  $[\text{Cu}_4(\text{O}_2\text{CC}_6\text{H}_5)_4]$  ( $[\text{Cu}_4]$ ) and  $[\text{Cu}_6(\text{O}_2\text{CC}_6\text{H}_5)_6]$  ( $[\text{Cu}_6]$ ), have been fully characterized in this work. While the  $[\text{Cu}_4]$  structure was previously reported, new features of its solid-state packing have been revealed, which assisted in rationalizing the photoluminescent trends for the  $[\text{Cu}_4]$  core based carboxylate series. The structure of  $[\text{Cu}_6]$  is reported here for the first time and adds the second example of a hexanuclear core copper(I) carboxylate having no exogenous ligands. The use of powder X-ray diffraction allowed us to detect a temperature induced phase transition for  $[\text{Cu}_6(\text{O}_2\text{CC}_6\text{H}_5)_6]$ . Both low and room temperature phases were studied by single crystal X-ray diffraction to reveal some minor differences in packing of the hexacopper(I) units.

The reversible  $[\text{Cu}_4] \leftrightarrow [\text{Cu}_6]$  core interconversion found in this system represents a unique example for the copper(I) carboxylate family. It was revealed only after different crystal growth conditions have been tested and successfully yielded variable crystalline products for a given metal–ligand combination. These variations in experimental conditions are very important in controlling the nuclearities and solid-state structures of copper(I) clusters, which is the key in affecting their properties, such as photoluminescence.

## Experimental Section

**Materials and Methods.** All manipulations were performed under a dinitrogen atmosphere employing standard Schlenk techniques. Sublimation–deposition procedures were carried out in small Pyrex glass ampules of 1.1 cm o.d. and of varied length (5–8 cm). The ampules were evacuated to ca.  $10^{-2}$  Torr, sealed, and then placed in electric furnaces having a ca. 5 °C temperature gradient along the length of the tube.  $[\text{Cu}_4(\text{O}_2\text{CCF}_3)_4]$  was synthesized following a previously reported procedure.<sup>7</sup> Benzoic acid, 99%, was obtained from Acros. Copper(I) oxide, 97%, and trifluoroacetic anhydride, 99%,

(32) (a) Hardt, H. D.; Weber, P. Z. *Anorg. Allg. Chem.* **1978**, *442*, 225–229. (b) Weber, P.; Hardt, H. D. *Inorg. Chim. Acta* **1982**, *64*, L51–L53.

(33) (a) Shin, C. H.; Huh, J. O.; Lee, M. H.; Do, Y. *Dalton Trans.* **2009**, 6476–6479. (b) Kumar, N. S. S.; Varghese, S.; Suresh, C. H.; Rath, N. P.; Das, S. J. *Phys. Chem. C* **2009**, *113*, 11927–11935.

were received from Sigma-Aldrich. All solvents (*m*-xylene, anhydrous, 99+%; benzene, anhydrous, 99.8%; 1,2-dichlorobenzene, anhydrous, 99%; hexanes, mixture of isomers, anhydrous, 99%) were purchased from Sigma-Aldrich and used as received.

**Physical Measurements.** Elemental analyses were performed by Guelph Chemical Laboratories Ltd., Canada. The room temperature photoluminescence (PL) spectra of crystalline powders were collected on a HORIBA Jobin Yvon spectrofluorimeter using front-face detection. Three full scans were recorded in each case and then averaged. Default hardware settings (the slit width of 2 nm and integration time of 0.2 s) were applied. The solid-state variable temperature PL spectra from fine powder of  $[\text{Cu}_6(\text{O}_2\text{CC}_6\text{H}_5)_6]$  (**2**) were recorded in the range of 300–900 nm using the custom-made liquid  $\text{N}_2$  filled cryostat with  $90^\circ$  detection geometry (Supporting Information, Figure S18) that was designed to work on a Shimadzu RF-5301 PC spectrofluorimeter. The temperature range was varied from  $-90$  to  $0^\circ\text{C}$  with the accuracy of temperature monitoring during spectra recording better than  $2^\circ\text{C}$ . Complex **2** was found to be a very bright emitter regardless of the wavelength in UV and visible region used for the excitation. Thus, the selected value of  $\lambda_{\text{ex}} = 260$  nm was the closest to the visible range wavelength that allowed recording of an untruncated signal using this particular instrument. Only at  $\lambda_{\text{ex}} = 260$  nm with the hardware settings of 1 nm minimal slit width, sampling interval of 1 nm, and a sampling time of 0.5 s, the recorded PL spectra would fit the vertical scale of the employed Shimadzu RF-5301 PC instrument. Actual photographs of **2** under UV-light are shown in Figure S19. The IR spectra were recorded on a Perkin-Elmer FT-IR Spectrometer (Spectrum 100) in the  $4000$ – $600\text{ cm}^{-1}$  range, using a universal ATR accessory. The Raman spectroscopic measurements were performed on an InVia Raman Microscope (Renishaw) using 785-nm laser light excitation. The GRAMS/AI software package (Thermo Galactic) was used for the spectroscopic data processing.

**Synthesis of  $[\text{Cu}_4(\text{O}_2\text{CC}_6\text{H}_5)_4]$  (**1**).** Benzoic acid (2.5 g, 10.24 mmol) was heated under reflux in 40 mL of *m*-xylene for 2 h with a Dean–Stark trap attached to the flask. The resulting solution was added to copper(I) oxide (0.2 g, 1.40 mmol) and reflux was continued until all the oxide had reacted (ca. 12 h). The solution was then slowly cooled to room temperature, and the white precipitate was filtered off. The polycrystalline powder was washed three times with *m*-xylene (20 mL) and dried under reduced pressure. Yield: 0.387 g, 75%. Anal calc for  $\text{C}_7\text{H}_5\text{O}_2\text{Cu}$ : C, 45.53; H, 2.73; O, 17.33. Found: C, 45.83; H, 2.71; O, 16.95%. PL ( $\lambda_{\text{ex}} = 418$  nm,  $\lambda_{\text{max}}$ , nm) 676. IR ( $\nu_{\text{max}}/\text{cm}^{-1}$ ): 3065s, 3028w, 1622w, 1594s, 1534s, 1492s, 1410s, 1314m, 1279w, 1173m, 1096w, 1069m, 1024m, 1003w, 976w, 936w, 843m, 811w, 705s, 690s, 678s. Raman ( $\nu_{\text{max}}/\text{cm}^{-1}$ ): 117w, 146w, 182w, 205w, 217w, 617m, 808w, 845s, 1004vs, 1027m, 1147m, 1161m, 1181m, 1425s, 1497m, 1602s, 3070w.

The X-ray powder pattern for this product was consistent with the calculated pattern for **1** based on the single crystal unit cell parameters (Supporting Information, Figure S9). To obtain single crystals of  $[\text{Cu}_4(\text{O}_2\text{CC}_6\text{H}_5)_4]$ , 0.040 g of the above powder was suspended in 10 mL of 1,2-dichlorobenzene and stirred at room temperature for 2 h. The saturated solution was filtered off (leaving ca. 0.020 g of an undissolved solid) and layered with 5 mL of hexanes. Upon hexane diffusion, colorless elongated plates appeared at the bottom of the flask. The solution was then carefully removed by cannula, and the resulting crystals were washed two times with *m*-xylene (5 mL) and dried under vacuum for 2 days. Yield: 0.011 g, 55% (based on the dissolved amount of solid). Several crystals from the precipitate were analyzed by single-crystal X-ray diffraction, and all conformed to those previously reported by Edwards<sup>12</sup> for

$[\text{Cu}_4(\text{O}_2\text{CC}_6\text{H}_5)_4]$ . The X-ray powder spectrum of the microcrystalline bulk material was fully consistent with the calculated powder pattern based on the single crystal unit cell parameters of **1** (Figure S5).

**Synthesis of  $[\text{Cu}_6(\text{O}_2\text{CC}_6\text{H}_5)_6]$  (**2**).** Crystals of **2** were obtained by sublimation ( $T_{\text{subl}} = 230^\circ\text{C}$ ) of the  $[\text{Cu}_4(\text{O}_2\text{CC}_6\text{H}_5)_4]$  powder prepared as described above. Yield of **2** is 35–40% after 12 h and 70–75% after 2 weeks of sublimation. Anal calc for  $\text{C}_7\text{H}_5\text{O}_2\text{Cu}$ : C, 45.53; H, 2.73; O, 17.33. Found: C, 45.25; H, 2.45; O, 17.69%. PL ( $\lambda_{\text{ex}} = 350$  nm,  $\lambda_{\text{max}}$ , nm) 577. IR ( $\nu_{\text{max}}/\text{cm}^{-1}$ ): 3062s, 3025w, 1620w, 1592s, 1543s, 1491s, 1410s, 1313m, 1279w, 1169m, 1095w, 1066m, 1024m, 1003w, 975w, 930w, 843m, 811w, 704s, 690s, 678s. Raman ( $\nu_{\text{max}}/\text{cm}^{-1}$ ): 118w, 152w, 182w, 207w, 219w, 616m, 813w, 844s, 1003vs, 1025m, 1143m, 1164m, 1181m, 1418s, 1493m, 1599s, 3070w. The X-ray powder spectrum of the microcrystalline bulk sample was fully consistent with the calculated powder pattern based on the single crystal unit cell parameters for **2**<sub>293K</sub> (Figure S7 of the Supporting Information).

**Transformation of  $[\text{Cu}_4(\text{O}_2\text{CC}_6\text{H}_5)_4]$  to  $[\text{Cu}_6(\text{O}_2\text{CC}_6\text{H}_5)_6]$ .** Crystals of **1** (0.035 g) obtained by recrystallization from 1,2-dichlorobenzene as described above were sublimed in an evacuated glass ampule at  $230^\circ\text{C}$ . The heating was stopped after 12 h, and crystals of  $[\text{Cu}_6(\text{O}_2\text{CC}_6\text{H}_5)_6]$  were collected from the walls of the ampule as colorless blocks. Yield: 0.015 g, 41%.

**Transformation of  $[\text{Cu}_6(\text{O}_2\text{CC}_6\text{H}_5)_6]$  to  $[\text{Cu}_4(\text{O}_2\text{CC}_6\text{H}_5)_4]$ .** Crystals of **2** (0.032 g) were suspended in 5 mL of 1,2-dichlorobenzene, and the mixture was stirred for 2 h at rt. The saturated solution was filtered off (leaving 0.021 g of an undissolved solid) and carefully layered with 5 mL of hexanes. In two days, colorless crystals of  $[\text{Cu}_4(\text{O}_2\text{CC}_6\text{H}_5)_4]$  appeared at the bottom of the tube. Yield: 0.009 g, 83% (based on the dissolved solid).

**X-ray Structural Determinations.** The X-ray data sets were collected for **1** and **2** on a Bruker APEX CCD X-ray diffractometer equipped with a graphite monochromated  $\text{Mo K}\alpha$  radiation source ( $\lambda = 0.71073\text{ \AA}$ ). Data reduction and integration were performed with the software package SAINT,<sup>34</sup> and absorption corrections were applied using the program SADABS.<sup>35</sup> All structures were solved and refined using the SHELXTL program package.<sup>36</sup> All non-hydrogen atoms were refined anisotropically. Hydrogen atoms were included at idealized positions as a riding model. Details on crystallographic data and experimental conditions for copper(I) benzoates are collected in Table 2. Crystallographic data for the single-crystal-to-single-crystal phase transition are shown in Table S1 (Supporting Information).

**Acknowledgment.** We thank the National Science Foundation for partial financial support (CHE-0546945) and for funding the X-ray powder diffractometer (CHE-0619422). We are very grateful to the University at Albany for supporting the X-ray center at the Department of Chemistry. We also thank Mr. Vitali Sikirzhyski (Prof. Lednev's group, University at Albany) for recording Raman spectra, and Dimitri Vaughn II and Beth Weaver for assistance in synthesis of copper(I) benzoate complexes during their undergraduate research study at the University at Albany.

**Supporting Information Available:** IR and Raman studies, X-ray powder diffraction details, X-ray data, TGA/DSC details, and PL data. This material is available free of charge via the Internet at <http://pubs.acs.org>.

(34) SAINT, version 6.02; Bruker AXS, Inc.: Madison, WI, 2001.

(35) SADABS; Bruker AXS, Inc.: Madison, WI, 2001.

(36) Sheldrick, G. M. SHELXTL, version 6.14; Bruker AXS, Inc.: Madison, WI, 2001.